Sublattice Localized Electronic States in Atomically Resolved Graphene-Pt(111) Edge-Boundaries

Pablo Merino,[†,^] Lucía Rodrigo,[‡,^] Anna L. Pinardi,[§] Javier Méndez,[§] Maria Francisca López,[§] Pablo Pou,[‡,⊥] Rubén Pérez,[‡,⊥] and Jose Angel Martín Gago[†,§,*]

[†]Centro de Astrobiología INTA-CSIC, Carretera de Ajalvir, km.4, E-28850 Madrid, Spain, [‡]Departamento de Física Teórica de la Materia Condensada, Universidad Autónoma de Madrid, E-28049 Madrid, Spain, [§]Instituto de Ciencia de Materiales de Madrid CSIC, C. Sor Juana Inés de la Cruz 3, E-28049 Madrid, Spain, and [⊥]Condensed Matter Physics Center (IFIMAC), Universidad Autónoma de Madrid, E-28049 Madrid, Spain. [^]These authors contributed equally.

ABSTRACT Understanding the connection of graphene with metal surfaces is a necessary step for developing atomically precise graphene-based technology. Combining high-resolution STM experiments and DFT calculations, we have unambiguously unveiled the atomic structure of the boundary between a graphene zigzag edge and a Pt(111) step. The graphene edges minimize their strain by inducing a 3-fold edge-reconstruction on the metal side. We show the existence of an unoccupied electronic state that is mostly localized on the C-edge atoms of one particular graphene sublattice, which could have implications in the design of graphene based devices.

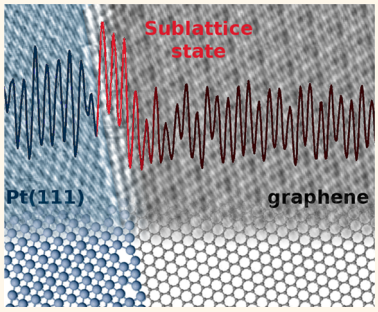

KEYWORDS: graphene nanoribbons · metal contacts · STM · DFT · electronic structure

The exceptional electronic properties of exotic graphene structures with low dimensionality have recently attracted the attention of the scientific and technological community as possible basic components in future atomically controlled graphene-based nanoelectronics.[1−3] The breaking of the perfect 2D periodicity of graphene in the presence of topological defects or in strain relief structures modifies significantly its electronic properties.[4,5] In particular, graphene nanobubbles have been suggested to present pseudomagnetic associated landau-levels,[2] and electronic one-dimensional edge states have been revealed to be localized in graphene nanoribbons.[6] These recently developed nanoarchitectures could open the door to tune the electronic transport of graphene-based electronic devices by ribbon or boundary engineering.

1D extended structures in Graphene are central to this effort.[3,7] The electronic structures of grain boundaries of polycrystalline graphene,[8] graphene nanoribbons (GNRs),[9,10] or edges have been extensively studied.[11,12] Theory predicts that the edges electronic properties can be tuned by the orientation of their ending (zigzag, armchair, mixed), possible reconstructions (pentagonal, heptagonal and higher order rings), and their chemical functionalization (normally H passivation).[10−14] Electron microscopy experiments were the first to provide a structural characterization of graphene edges with atomic resolution using either aberration-corrected TEM images[15] or scanning transmission electron microscope (STEM).[16] Recent dynamic atomic force microscopy (AFM) studies have presented this technique as an ideal tool to the study of atomically precise carbon nanostructures[7,17,18] Scanning tunneling microscope (STM) measurements performed on graphene patches deposited on different substrates[6,19,20] added the possibility to correlate the structure with the local electronic properties. Even though atomic resolution was achieved in those experiments, STM was unable to reveal the details of the edge termination due to the interaction with the substrate. STM experiments based on graphene islands grown directly on a metallic substrate[21,12] offer the possibility to study not only the edges "flying freely" on the lower

* Address correspondence to Gago@icmm.csic.es.

Received for review January 7, 2014 and accepted March 21, 2014.

Published online March 21, 2014
10.1021/nn500105a

substrate terrace (*step-like* edges) but also those bound to the upper terrace of the substrate (*border-like* edges). Although these studies were able to show a correlation between the atomic corrugation at the graphene edges and the Moiré pattern of G/Ir, where the absence of electronic G-edge states has been reported,[13] an atomically precise description of graphene contacts with metallic substrates is still missing.

In this work we provide the first combined experimental and theoretical atomistic description of the in-plane contact region formed along the 1D interface in a graphene–metal heterostructure and unveil its electronic properties. We have been able to obtain high-resolution room temperature STM images of atomically resolved *border-like* edges of graphene on Pt(111) steps. We have combined these detailed experimental results with DFT simulations to fully characterize the atomic structure of the Pt-graphene edges, which allow us to understand their electronic properties. Our results contrast with the ones obtained for the G/Ir edges system,[13] as we reveal the presence of 1D electronic states that are highly localized exclusively in one of the graphene sublattices. Theory predicts, and STM images confirm, that this state is mainly confined on the first lines of carbon atoms of the edge. This state is very robust and despite the thermal broadening it is possible to observe it even using a room temperature STM instrument. This combination of sublattice and edge localization would make possible the design of a dual-channel device based on a graphene nanoribbon contacted with two different border-like edges.

Moreover, our results also shed light on the role of the substrate steps in the nucleation and formation of different Moiré patterns on metal surfaces. The characterization of the particular periodicities found in these superstructures and their possible origin have been subjected to numerous studies (see[5,22,23] and references therein). Here we present an atomic-scale description of the bonding arrangements at the interface between a Pt(111) step and a graphene island that brings a deeper understanding of this point. Our results show that graphene nucleates on the Pt steps inducing a 1D reconstruction on the Pt atoms, which are coupled to graphene ending in a zigzag configuration. We exploit these observations to show that the precise structure of these edges is responsible for originating the particular orientation of the formed Moiré patterns (see Supporting Information).

RESULTS AND DISCUSSION

The constant current STM image on Figure 1A shows a graphene island (represented in gray color) which grows attached to the upper part of a Pt(111) step. The usually straight Pt step-edge has been altered from its original shape during the graphene growth. In this image, approximately half of the graphene island is embedded in the upper terrace (with respect to the Pt steps), adjusting itself to the crystallographic directions of

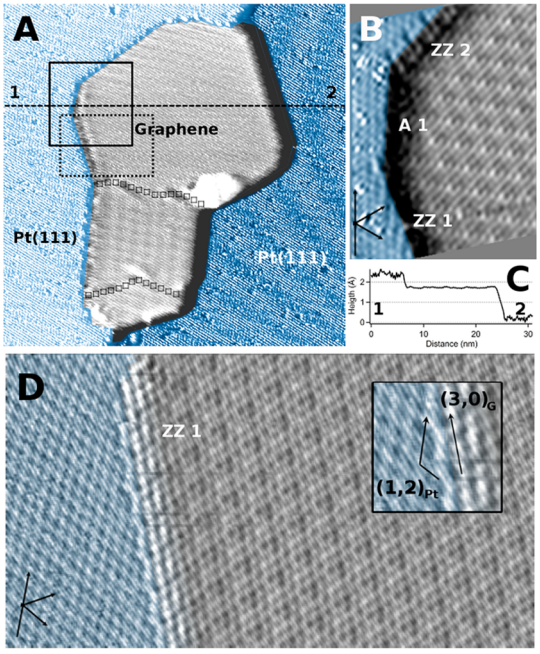

Figure 1. (A) Constant current STM image (31 × 31 nm^2, sample voltage V_s = 100 mV, tunneling current I_t = 3.9 nA) showing a graphene island embedded in a Pt(111) terrace exhibiting three different Moirés; the graphene–graphene edges between Moires are represented with squared lines overimposed. (B) Drift corrected quasi-constant height STM image (6 × 8 nm^2, V_s = 42 mV, I_t = 2.5 nA) displaying a detailed view of three border-like edges of the solid black squared region in (A). Black arrows indicate the [1$\bar{1}$0] and equivalent Pt crystallographic directions. (C) Profile recorded in topographic mode corresponding to the dashed line marked in (A). (D) high-resolution, unfiltered, atomically resolved, quasi-constant current STM image of the ZZ1 edge corresponding to the pointed line rectangle marked in (A) (12.6 × 6.8 nm^2, V = 40.2 mV, I = 5.2 nA). The inset shows the surface crystallographic vectors of the edge and graphene structures with respect to the surface vectors of the Pt(111) (suffix Pt), and respect to the surface vectors of graphene (suffix G). All images have the same scanning direction, which is parallel to the horizontal.

the substrate. This morphology indicates significant mass transport of Pt atoms during graphene growth and differs from the structures reported for graphitization on other metal surfaces, such as Ir(111)[24,20] or Ru(0001),[25] where graphene normally grows over the metal steps without altering the metal substrate.

Three different rotational domains of graphene separated by nonperiodic grain boundaries can be clearly identified in the island of Figure 1A (see squared lines). The upper domain is rotated 19.1° with respect to the surface [1$\bar{1}$0] crystallographic surface direction, which in the image runs parallel to the vertical direction, and it exhibits a superstructure periodicity of 7.38 Å. This graphene superstructure is usually denoted as ($\sqrt{7} \times \sqrt{7}$)R19°, with respect to the Pt(111) surface, $(3 \times 3)_G$, with respect to the graphene surface vectors, or βG/Pt(111), according to the notation introduced in ref 23. The middle domain is rotated 8° and presents a periodicity of 13 Å; it most likely corresponds to ($\sqrt{31} \times \sqrt{31}$)R9° or εG/Pt(111). Finally, the lowest

domain is small in size and we were not able to attain Moiré resolution to deduce the graphene orientation.

The upper ($\sqrt{7} \times \sqrt{7}$)R19° domain of Figure 1A exhibits a polygonal shape with four *border-like* and three *step-like* edges.[21] STM topographic profiles (see Figure 1C) confirm the existence of both G-metal boundaries, showing different height jump decay for border-like and step-like edges. The atomic resolution at the border-like edge strongly depends on the tip termination. Although in some cases, as the one shown in Figure 1D (corresponding to the pointed-line rectangle in the Figure 1A), the resolution is very good, this is not a usual case. To routinely enhance the resolution at the G-Pt boundaries, we have recorded quasi-constant height STM images (showing the difference between the current set-point and the actual current measured in each point recorded during the conventional STM operation with the feedback on). Both STM topographic and quasi-constant height images show the same atomic features on the same positions, but the atomic resolution at both sides of the step is strongly enhanced, as it is shown in Figure 1D and in the Supporting Information. The improved resolution at the edge is also clearly illustrated in Figure 1B where the quasi-constant height STM images exhibit atomic resolution not only on the Pt(111) terrace and the island but also at the interface.

Interestingly, some of these edges maintain a crystallographic relationship with the Pt substrate. This is the case of the edge shown in the constant-current image of Figure 1D, where long-range order is appreciated at the interface between Pt and graphene. The inset shows the crystallographic vectors with respect to the surface unit cell of Pt(111). High-resolution STM images allow a systematic characterization of all of the different border-like edges on the ($\sqrt{7} \times \sqrt{7}$)R19° graphene Moiré shown in Figure 1. These results are shown in Figure 2, where edges have been labeled as ZZ (for a zigzag graphene ending) and A (for an amorphous or armchair configuration). Border A1 is parallel to the [1$\bar{1}$0] Pt crystallographic direction, while borders ZZ1 and ZZ2 run along the [3$\bar{2}\bar{1}$] and [1$\bar{3}$2] directions, respectively, forming 19° and 41° with the [1$\bar{1}$0] direction. A1 and A2 edges present a disordered structure with two different independent atomic structures (for example, A2 border presents a mixture of armchair and zigzag termination), whereas the other two edges, ZZ1 and ZZ2, are crystalline.

Most atomically resolved edges show regions that can be unambiguously assigned to Pt and G (blue and gray colored areas on Figure 2, respectively) and a boundary area of 3 to 4 atomic rows, where the atoms although clearly visible cannot be directly ascribed to a particular chemical element (gradient colored area). As a result of *ab initio* simulations based on DFT for a graphene flake attached to a Pt step (see Supporting Information for details), a much deeper understanding of these edges can be achieved. Figure 3 shows the main results of these

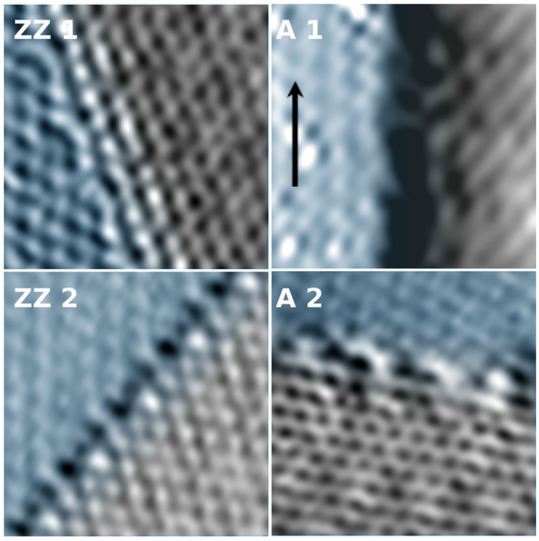

Figure 2. Atomically resolved quasi-constant height STM images (2.5 × 2.5 nm^2) of (ZZ1) the zigzag edge number 1, I_t = 5.2 nA, V_s = 38 mV; (A1) the amorphous edge number 1, I_t = 2.4 nA, V_s = 42 mV, the arrow indicates the Pt [1$\bar{1}$0] direction; (ZZ2) the zigzag edge number 2, I_t = 3.8 nA, V_s = 47 mV; and (A2) the amorphous edge number 2, I_t = 5.2 nA, V_s = 38 mV. Blue/gray regions are identified by the lattice symmetry to be Pt/G, respectively. A boundary region of 3 to 4 atomic rows is also clearly observed with atomic resolution. These images have been drift corrected and FFT filtered.

calculations. Starting from different initial structures for the G-Pt interface, we have obtained a stable configuration where the stress induced in the G−Pt junction has been relaxed with a rearrangement of the outermost Pt atoms of the single-atom step (see Figures 3A,B). The unit cell of our system involves three nonequivalent Pt atoms directly bonded to graphene. To ease the visualization, we have marked them with blue, red, and green colors. These Pt atoms undergo both out-of and in-plane displacements. The red Pt atom on Figure 3 protrudes 0.65 Å out of the Pt terrace plane and it moves in plane from its original position ∼1 Å toward the graphene forming a bond with an unsaturated C edge atom. As a result, a hole is created on the Pt side. This can be visualized in Figure 3A as the vacant region beneath the red Pt atom. The blue and green Pt atoms also passivate one outermost C atom each, but they show lower strains and displacements, and the more significant is the −0.15 Å out-of-plane displacement (inward relaxation) of the blue atom on Figure 3.

This atomic structure mimics with great accuracy the atomically resolved experimental STM images (see Figure 3C) for the ZZ edge. The strain induced on the Pt side is localized mainly on the outermost Pt atoms and only slightly propagate to the second Pt row. While free-standing zigzag edges should undergo reconstruction, no relevant rearrangement is observed on the graphene side in our results. The external C atoms of the zigzag edge are covalently bonded to the metal step, keeping their graphene-like positions. This covalent interaction between graphene and Pt, already

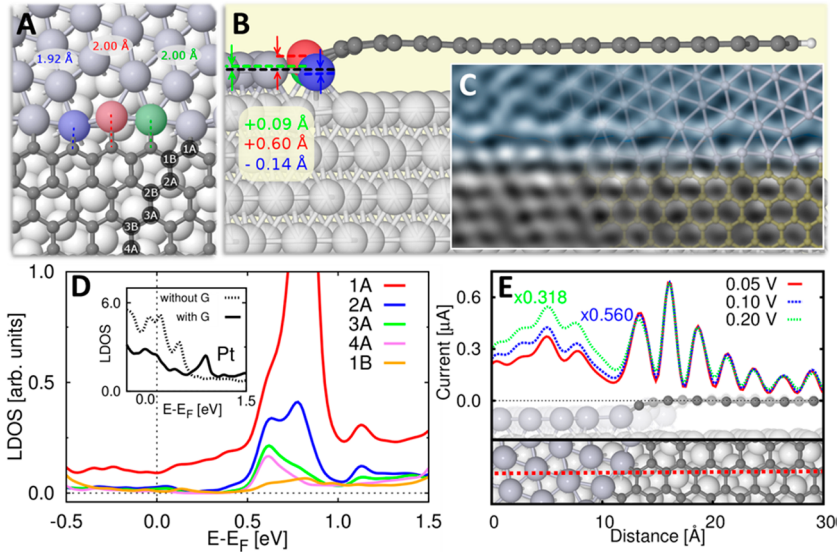

Figure 3. (A and B) Ball-and-stick model of the atomic configuration of graphene on the Pt(111) step edge calculated with DFT. Bond distance (A) and out of plane displacement (B) of the Pt edge atoms are indicated. (C) Quasi-constant height STM image (3.5 × 1.6 nm^2) and overlay of the calculated structure for edge ZZ1. (D) Local density of states (LDOS) for the 1st (red), 2nd (blue), 3rd (green), and 4th (pink) rows of C atoms belonging to the same sublattice and for the 1st (orange) one of the other sublattice. An electronic state at approximately +0.8 eV above E_F is clearly observed only in one sublattice and is mainly localized on the edge row. This state extends into the Pt row in direct contact with the graphene, as shown in the inset, where the theoretical LDOS of this Pt row is shown with and without the graphene flake. The electronic state at approximately +0.8 eV appears in the case of the complete system while it is missing in the isolated metal. (E) Theoretical constant-height STM simulations of a profile through one of the A-sublattice lines depicted below in both side view and top view where the line profile is highlighted by a dashed red line. Currents at a tip−sample distance of 2.75 Å with respect to the uppermost atom in the cell including multiple scattering contributions for 0.05 V (red), 0.10 V (green), and 0.20 V (blue) bias voltages are shown. The rescaling of the profiles for 0.10 and 0.20 V allow us to check that the behavior is not affected by the voltage used.

theoretically proposed for Cu, Co, and Ni(111) surfaces[26−28] and observed with STM on G/Ir,[21] passivates the graphene dangling bonds and stabilizes the zigzag structure.[27] Our calculations have found another stable configuration for the boundary where the stress is relaxed on the graphene edge instead of on the Pt side. The match between this theoretical structure and the STM experimental images for ZZ1 and ZZ2 edges is clearly worse (see Figure S6 in the Supporting Information), and we have not considered it further.

The precise determination of the atomic structure of the G-Pt boundaries sheds light on the geometry of the stable Moiré patterns reported for Pt(111).[23] Our results show that these superstructures can be correlated with the crystallographic edges of the graphene islands formed during their growth (see Supporting Information). Rotational domains nucleate on the Pt step, binding the graphene island with the metal substrate with one of the particular orientations that produce energetically favorable border-like ZZ boundaries, and then continuing its growth with that angle. The link between the stability of the Moiré and the energetic of the edge boundary is supported by the STM analysis of different graphene islands. The observed Moiré patterns have grown following particular orientations that maximize the number of zigzag graphene terminations (see Supporting Information) and the G−Pt edges tend to be parallel to the apparent angle of the Moiré superstructure.

The good match between the calculated atomic structure and the experimental STM images also motivates us to characterize the electronic structure at the edges by calculating the local density of states (LDOS) associated to this nanostructure. Figure 3D shows the calculated LDOS for the first carbon rows. A localized state about +0.8 eV above the Fermi level, with a fwhm of 0.2 eV, is found at the carbon atoms bonded to Pt. This state decays strongly in intensity when moving away from the edge. Furthermore, it is mainly localized in one sublattice: the LDOS of the neighboring C atoms (orange curve in Figure 3D), belonging to the other sublattice, does not show any trace of this state. Free-standing graphene edges are characterized by the presence of a localized state at the Fermi level. In our case, both the charge transfer between the flake and the metal and the strong G−Pt interaction broaden this peak and shift it toward positive energies resulting in the peak that we observe at about +0.8 eV. Its position with respect to the Fermi level and its decay length (~6 Å) are similar to the ones associated with a single atom vacancy on graphene on Pt.[29] As in this case, the magnetic moments associated with the G-edge in free-standing graphene are quenched due to the interaction with the metal. Looking at the Pt side of the edge, we have found that the LDOS projected on the Pt row closer to the interface shows a peak at the same E_F +0.8 eV energy. This peak is not present in the LDOS of the pristine Pt step, indicating that the G-edge

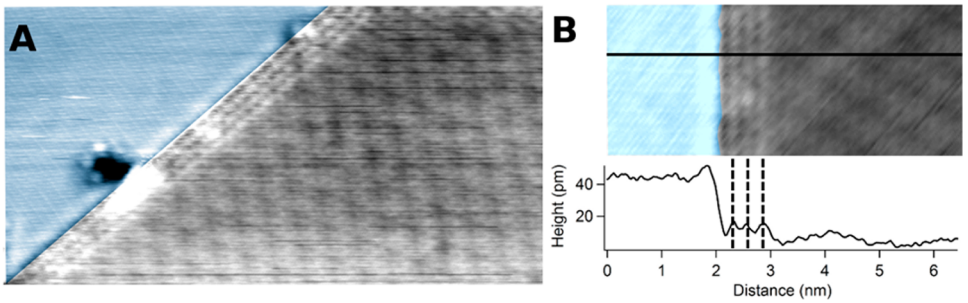

Figure 4. (A) Constant current STM image (13.4 × 6.9 nm^2) of a border-like edge where an excess of charge is visualized parallel to the interface in the first three rows of graphene, V_s = 51 mV, I_t = 4 nA. (B) Detail of such 1D states and height profile.

state spreads out inside the Pt (see Figure 3D and Figure S3 on Supporting Information).

This result contrast with that of ref 13 where the authors show that the edge states at Ir(111) are quenched by the strong interaction between the metal and the graphene. In this case, the graphene edges are hybridized with the substrate. The graphene−metal interaction is much stronger than that in Pt, and therefore, it is able to modify the sp^2 hybridization of the edge-C atoms and to block the edge-state.

The presence of the G-edge has a profound influence not only for energies around the edge state at about +0.8 eV but also in a wider energy range, including the Fermi level. Our calculated LDOS at zero energy shows similar spatial decay found for the main peak (see Figure S4 in Supporting Information). Low bias STM images should display this behavior and this is indeed what we observe. Constant height STM simulations of a line profile scanning the A-graphene sublattice, the one whose atoms are in direct contact with the metal, show the decay of the electronic states associated to the G-edge for energies close to the Fermi level (see Figure 3E). The periodic protrusions decaying in intensity as we move into the graphene layer are the most characteristic attributes. In Figures 1D and 4A, we show experimental STM images where a modulation of the signal parallel to the border-like edge is clearly visualized. The distance between the maxima of the atomic lines is 2.4 Å (see the height profile in Figure 4B). This value corresponds to the distance of equivalent atoms in the graphene network and indicates that the edge state is mainly confined in one of the two sublattices. This state, decaying away from the interface and localized in one of the sublattices, is also visible in the STM image of the ZZ1 edge in Figure 2. STM images of different edges show that, typically, after 4 atomic lines the state fully disappears.

Interestingly, this state is localized both in energy and real space. It vanishes as we move out of the interface. Therefore, they can be considered as 1D electronic states associated to each of the graphene sublattices. These electronic states confined in specific sublattices of the graphene structure open new opportunities to future atomically precise graphene based electronics and valleytronics.[30,31] For instance, new multichannel nanowires could be built by contacting the opposite sides of a graphene flake with two different border-like edges. We speculate that these atomically precise nanoleads will excite, respectively, each one of the two graphene sublattices, allowing two-ways atomically controlled transport *via* these independent electronic states (see Supporting Information).

CONCLUSIONS

We present a combined STM and DFT study of edge heterostuctures of graphene grown on Pt(111) in which we disclose the atomic structure of the G−Pt boundary. The unsaturated C atoms strongly interact with the Pt step, preserving a zigzag structure quite close to the ideal configuration. However, on the other side, Pt edge atoms experience a 3-fold reconstruction that stabilizes the structure. The tendency to form passivated zigzag graphene terminations plays a relevant role in the formation and orientation of the stable Moiré patterns. Our combined approach reveals the interesting electronic properties of this nanoscopic system including, as stated by the simulations, the preservation of the G-edge state shifted to energies at about +0.8 eV above Fermi level, highly localized in one of the graphene sublattices and confined to the G−Pt interface. This state spreads out inside the first Pt row resulting in a high quality G−metal electric contact that could be relevant for designing future atomically precise graphene metal leads.

METHODS

Experiments were carried out in an ultrahigh vacuum (UHV) chamber with base pressure of 1 × 10^{-10} mbar. The Pt(111) single crystal sample was cleaned by repeated cycles of Ar^+ sputtering and subsequent annealing at 1200 K. After several cycles, the sample purity was checked with low energy electron diffraction (LEED) and STM. To grow graphene, we exposed the clean Pt(111) to a partial pressure of propane (C_3H_8) of 1.1 × 10^{-8} mbar during 15 min keeping the sample at 900 K and subsequent anneal at 1050 K during 20 min. Submonolayer coverage of graphene islands was observed in the STM sessions with an estimated coverage of >0.1 ML. STM images were

acquired using a room temperature (RT) microscope. We used both topographic and quasi-constant height modes (see Supporting Information for more details) with typical biases of −250 to 250 mV and currents between 0.1 and 4 nA. WSxM software was used for data acquisition and image analysis. The thermal drift was corrected with a homemade program, which resized the images for a given hexagonal unit cell by keeping the fast scan axis as the reference distance.

DFT Calculations. We have calculated all the structural and electronic properties using DFT as implemented in the VASP code.[32] For these calculations, we employed the PBE functional empirically corrected to include van der Waals interactions (using the D2 Grimme approach) projector augmented wave (PAW) pseudopotentials, and a plane-wave cutoff of 400 eV. To build our theoretical system, we have combined a Pt step and a graphene flake attached right to the border of the step. The cell is repeated, as shown in the Supporting Information (Figure S2), to allow the simulation of a long graphene flake with a quite small unit cell. The cell includes a slab of 5 layers of Pt to which a single sheet of graphene (a 3 × 12 cell with 72 atoms) has been attached. The 4 lower Pt layers contain 28 atoms each, while the one on top has half the area of the others (14 atoms) and the graphene layer is bonded to its free edge. To make the electronic properties of the flake more realistic, we have saturated the other border with 3 H atoms. This edge does not pretend to mimic any border of the simulated experiments. Calculations with a flake half the length of the one in Supporting Information Figure S2 confirm that the structural properties of the G−Pt boundary are not significantly affected by the flake length. The unit cell vectors do not only displace the cell in *x*- and *y*-directions but also in the *z*-direction to be able to simulate the step and to reproduce the ABC stacking (see Supporting Information Figure S2). The mismatch between the C and Pt lattices in the 3 × 3 Moiré of G/Pt(111) is small (0.6%), and in our calculations, we decided to fix the size of the supercell to match the relaxed graphene lattice (a_0 = 2.46 Å). See Supporting Information for more details.

Conflict of Interest: The authors declare no competing financial interest.

Acknowledgment. We thank M. Švec for fruitful discussion and development of the code used for correcting the drift. We acknowledge financial support from Spanish Grants MAT2010-17720, MAT2011-23627, MAT2011-26534, CSD2008-00041, CSD2010-00024, PLE2009-0061 (MINECO, Spain) and S2009/MAT-1467 (CAM, Spain). The research leading to these results has received funding from the European Union Seventh Framework Programme under Grant agreement No. 604391 Graphene Flagship. P.P. and P.M. were supported by the Ramón y Cajal and "Rafael Calvo Rodés" programs, respectively. Computer time provided by the Spanish Supercomputing Network (RES) in the Barcelona Supercomputer Center (MareNostrum III) is gratefully acknowledged.

Supporting Information Available: Materials and methods; details of the electronic structure of the G−Pt step boundary; an alternative configuration of the G−Pt step boundary found in the calculations; crystalline borders and their relation with Moiré patterns; possible design of an hypothetical dual channel nanoribbon; complete list of references. This material is available free of charge *via* the Internet at http://pubs.acs.org.

REFERENCES AND NOTES

1. Lahiri, J.; Lin, Y.; Bozkurt, P.; Oleynik, I. I.; Batzill, M. An Extended Defect in Graphene as a Metallic Wire. *Nat. Nanotechnol.* **2010**, *5*, 326–329.
2. Levy, N.; Burke, S. A.; Meaker, K. L.; Panlasigui, M.; Zettl, A.; Guinea, F.; Neto, A. H. C.; Crommie, M. F. Strain-Induced Pseudo-Magnetic Fields Greater Than 300 T in Graphene Nanobubbles. *Science* **2010**, *329*, 544–547.
3. Wang, L.; Meric, I.; Huang, P.; Gao, Q.; Gao, Y.; Tran, H.; Taniguchi, T.; Watanabe, K.; Campos, L.; Muller, D. One-Dimensional Electrical Contact to a Two-Dimensional Material. *Science* **2013**, *342*, 614–617.
4. Nakada, K.; Fujita, M.; Dresselhaus, G.; Dresselhaus, M. S. Edge State in Graphene Ribbons: Nanometer Size Effect and Edge Shape Dependence. *Phys. Rev. B* **1996**, *54*, 17954–17961.
5. Batzill, M. The Surface Science of Graphene: Metal Interfaces, CVD Synthesis, Nanoribbons, Chemical Modifications, and Defects. *Surf. Sci. Rep.* **2012**, *67*, 83–115.
6. Tao, C.; Jiao, L.; Yazyev, O. V.; Chen, Y.-C.; Feng, J.; Zhang, X.; Capaz, R. B.; Tour, J. M.; Zettl, A.; Louie, S. G.; *et al.* Spatially Resolving Edge States of Chiral Graphene Nanoribbons. *Nat. Phys.* **2011**, *7*, 616–620.
7. Boneschanscher, M. P.; van der Lit, J.; Sun, Z.; Swart, I.; Liljeroth, P.; Vanmaekelbergh, D. Quantitative Atomic Resolution Force Imaging on Epitaxial Graphene with Reactive and Nonreactive AFM Probes. *ACS Nano* **2012**, *6*, 10216–10221.
8. Yazyev, O. V.; Louie, S. G. Electronic Transport in Polycrystalline Graphene. *Nat. Mater.* **2010**, *9*, 806–809.
9. Ruffieux, P.; Cai, J.; Plumb, N. C.; Patthey, L.; Prezzi, D.; Ferretti, A.; Molinari, E.; Feng, X.; Mullen, K.; Pignedoli, C. A.; *et al.* Electronic Structure of Atomically Precise Graphene Nanoribbons. *ACS Nano* **2012**, *6*, 6930–6935.
10. Yazyev, O. V. A Guide to the Design of Electronic Properties of Graphene Nanoribbons. *Acc. Chem. Res.* **2013**, *46*, 2319–2328.
11. Acik, M.; Chabal, Y. J. Nature of Graphene Edges: A Review. *Jpn. J. App. Phys.* **2011**, *50*, 070101.
12. Yamamoto, M.; Obata, S.; Saiki, K. Structure and Properties of Chemically Prepared Nanographene Islands Characterized by Scanning Tunneling Microscopy. *Surf. Interface Anal.* **2010**, *42*, 1637–1641.
13. Li, Y.; Subramaniam, D.; Atodiresei, N.; Lazić, P.; Caciuc, V.; Pauly, C.; Georgi, A.; Busse, C.; Liebmann, M.; Blügel, S.; *et al.* Absence of Edge States in Covalently Bonded Zigzag Edges of Graphene on Ir(111). *Adv. Mater.* **2013**, *25*, 1967–1972.
14. Chia, C.-I.; Crespi, V. H. Stabilizing the Zigzag Edge: Graphene Nanoribbons with Sterically Constrained Terminations. *Phys. Rev. Lett.* **2012**, *109*, 076802.
15. Girit, C. O.; Meyer, J. C.; Erni, R.; Rossell, M. D.; Kisielowski, C.; Yang, L.; Park, C. H.; Crommie, M. F.; Cohen, M. L.; Louie, S. G.; *et al.* Graphene at the Edge: Stability and Dynamics. *Science* **2009**, *323*, 1705–1708.
16. Suenaga, K.; Koshino, M. Atom-by-Atom Spectroscopy at Graphene Edge. *Nature* **2010**, *468*, 1088–1090.
17. Gross, L.; Mohn, F.; Moll, N.; Liljeroth, P.; Meyer, G. The Chemical Structure of a Molecule Resolved by Atomic Force Microscopy. *Science* **2009**, *325*, 1110–1114.
18. van der Lit, J.; Boneschanscher, M. P.; Vanmaekelbergh, D.; Ijäs, M.; Uppstu, A.; Ervasti, M.; Harju, A.; Liljeroth, P.; Swart, I. Suppression of Electron−Vibron Coupling in Graphene Nanoribbons Contacted *via* a Single Atom. *Nat. Commun.* **2013**, *4*, 2023.
19. Ritter, K. A.; Lyding, J. W. The Influence of Edge Structure on the Electronic Properties of Graphene Quantum Dots and Nanoribbons. *Nat. Mater.* **2009**, *8*, 235–242.
20. Ridene, M.; Girard, J. C.; Travers, L.; David, C.; Ouerghi, A. STM/STS Investigation of Edge Structure in Epitaxial Graphene. *Surf. Sci.* **2012**, *606*, 1289–1292.
21. Phark, S.-h.; Borme, J.; Vanegas, A. L.; Corbetta, M.; Sander, D.; Kirschner, J. Atomic Structure and Spectroscopy of Graphene Edges on Ir(111). *Phys. Rev. B* **2012**, *86*, 045442.
22. Wintterlin, J.; Bocquet, M. L. Graphene on Metal Surfaces. *Surf. Sci.* **2009**, *603*, 1841–1852.
23. Merino, P.; Švec, M.; Pinardi, A. L.; Otero, G.; Martín-Gago, J. A. Strain-Driven Moiré Superstructures of Epitaxial Graphene on Transition Metal Surfaces. *ACS Nano* **2011**, *5*, 5627–5634.
24. Coraux, J.; N'Diaye, A. T.; Engler, M.; Busse, C.; Wall, D.; Buckanie, N.; Heringdorf, F.-J. M. z.; Gastel, R. v.; Poelsema, B.; Michely, T. Growth of Graphene on Ir(111). *New J. Phys.* **2009**, *11*, 023006.
25. Marchini, S.; Günther, S.; Wintterlin, J. Scanning Tunneling Microscopy of Graphene on Ru(0001). *Phys. Rev. B* **2007**, *76*, 075429.
26. Gao, J.; Yip, J.; Zhao, J.; Yakobson, B. I.; Ding, F. Graphene Nucleation on Transition Metal Surface: Structure Transformation and Role of the Metal Step Edge. *J. Am. Chem. Soc.* **2011**, *133*, 5009–5015.

27. Gao, J.; Zhao, J.; Ding, F. Transition Metal Surface Passivation Induced Graphene Edge Reconstruction. *J. Am. Chem. Soc.* **2012**, *134*, 6204–6209.
28. Stokbro, K.; Engelund, M.; Blom, A. Atomic-Scale Model for the Contact Resistance of the Nickel-Graphene Interface. *Phys. Rev. B* **2012**, *85*, 165442.
29. Ugeda, M. M.; Fernández-Torre, D.; Brihuega, I.; Pou, P.; Martínez-Galera, A. J.; Pérez, R.; Gómez-Rodríguez, J. M. Point Defects on Graphene on Metals. *Phys. Rev. Lett.* **2011**, *107*, 116803.
30. Gunlycke, D.; White, C. T. Graphene Valley Filter Using a Line Defect. *Phys. Rev. Lett.* **2011**, *106*, 136806.
31. Rycerz, A.; Tworzydlo, J.; Beenakker, C. W. J. Valley Filter and Valley Valve in Graphene. *Nat. Phys.* **2007**, *3*, 172–175.
32. Kresse, G.; Furthmüller, J. Efficient Iterative Schemes for *ab Initio* Total-Energy Calculations Using a Plane-Wave Basis Set. *Phys. Rev. B* **1996**, *54*, 11169.